

SSL-GMMVC: Interpretable Voice Conversion via Locally Linear GMM Transforms in Self-Supervised Representation Space

Tomoya Tanabu¹, Hiroshi Nishijima¹, Daisuke Saito¹, Nobuaki Minematsu¹

¹ The University of Tokyo, Japan

{tanabu,hiroshi,dsk_saito,mine}@gavo.t.u-tokyo.ac.jp

Abstract

We introduce SSL-GMMVC, an interpretable voice conversion method in self-supervised speech space. The method models paired source-target features with a Gaussian mixture model and performs conversion as a posterior-weighted sum of affine transforms. This yields locally linear transformations that adapt to heterogeneous feature-space structure while remaining analytically tractable. Through objective and subjective evaluations, we show that SSL-GMMVC improves speaker similarity with comparable intelligibility and naturalness, and that even a constrained covariance variant surpasses a deep learning baseline as the number of mixture components increases. Further analyses link component selection to phonetic structure and reveal interpretable scaling and rotation in the learned transforms. These findings highlight SSL-GMMVC as an effective, analyzable framework for voice conversion.

Index Terms: voice conversion, self-supervised learning, gaussian mixture model

1. Introduction

Voice conversion (VC) modifies a speaker’s voice to sound like another person while preserving linguistic content [1]. Its applications include anonymization [2, 3], computer-assisted language learning [4, 5], and speaking aid [6, 7].

VC progress has been driven by advances in both transformation models and speech representations [8, 9]. Self-supervised learning (SSL) has yielded general-purpose acoustic embeddings, including wav2vec 2.0 [10], HuBERT [11], and WavLM [12], that transfer well across various downstream tasks [13–15]. Several VC systems, such as S3PRL-VC [16], FreeVC [17], and AdaptVC [18], now leverage these representations as input, yet still rely on complex neural architectures for the transformation itself.

At the same time, recent work suggests that competitive VC can arise from surprisingly simple operations on SSL features. kNN-VC [19] and LinearVC [20] show that nearest-neighbor replacement or a single linear mapping in SSL space can yield intelligible speech with target-speaker resemblance. However, a global linear transform cannot adapt to local structure that may vary across phonetic clusters [21], limiting its expressiveness.

To address this, we propose SSL-GMMVC¹, a Gaussian Mixture Model (GMM)-based VC operating on SSL representations. SSL-GMMVC replaces the single global mapping of LinearVC with a set of locally linear transformations, preserving interpretability while being more expressive. By focusing on simple, locally interpretable transformations in SSL space,

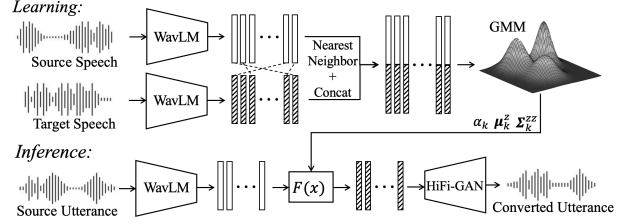


Figure 1: Overview of SSL-GMMVC

we aim to improve conversion performance and to better understand SSL embedding spaces.

2. SSL-GMMVC

2.1. Overview

We propose SSL-GMMVC, a GMM-based voice conversion system operating on SSL features. Figure 1 shows an overview of the pipeline. We align SSL features of source and target utterances using nearest-neighbor matching to obtain paired source–target vectors following [20], and model their joint distribution with a GMM. At conversion time, the learned parameters define an explicit function that maps source features to the target space, and a vocoder synthesizes waveforms from the converted features.

2.2. GMM-based voice conversion

Let $\mathbf{x}, \mathbf{y} \in \mathbb{R}^D$ denote frame-level SSL features of the source and target speakers. After alignment, we apply GMM-based voice conversion [22] by fitting a K -component GMM to the joint vectors $\mathbf{z} = [\mathbf{x}^\top, \mathbf{y}^\top]^\top \in \mathbb{R}^{2D}$:

$$p(\mathbf{z}) = \sum_{k=1}^K \alpha_k \mathcal{N}(\mathbf{z}; \boldsymbol{\mu}_k^z, \boldsymbol{\Sigma}_k^{zz}) \quad (1)$$

where α_k is a mixture weight, and $\boldsymbol{\mu}_k^z$ and $\boldsymbol{\Sigma}_k^{zz}$ are the mean and covariance of component k . We partition the mean and covariance into source and target blocks:

$$\boldsymbol{\mu}_k^z = \begin{bmatrix} \boldsymbol{\mu}_k^x \\ \boldsymbol{\mu}_k^y \end{bmatrix}, \quad \boldsymbol{\Sigma}_k^{zz} = \begin{bmatrix} \boldsymbol{\Sigma}_k^{xx} & \boldsymbol{\Sigma}_k^{xy} \\ \boldsymbol{\Sigma}_k^{yx} & \boldsymbol{\Sigma}_k^{yy} \end{bmatrix} \quad (2)$$

Learning. We estimate $\{\alpha_k, \boldsymbol{\mu}_k^z, \boldsymbol{\Sigma}_k^{zz}\}_{k=1}^K$ using the EM algorithm. The E-step computes the responsibility $p(k|\mathbf{z}_n)$ for each data point \mathbf{z}_n :

$$p(k|\mathbf{z}_n) = \frac{\alpha_k \mathcal{N}(\mathbf{z}_n; \boldsymbol{\mu}_k^z, \boldsymbol{\Sigma}_k^{zz})}{\sum_{m=1}^K \alpha_m \mathcal{N}(\mathbf{z}_n; \boldsymbol{\mu}_m^z, \boldsymbol{\Sigma}_m^{zz})} \quad (3)$$

¹Code public at: github.com/tomoya-san/ssl-gmmvc

The M-step updates mixture weights, means, and covariances, and we iterate until convergence.

Inference. Given a source feature \mathbf{x} , we compute the posterior of each component from the source-side marginal:

$$p(k|\mathbf{x}) = \frac{\alpha_k \mathcal{N}(\mathbf{x}; \boldsymbol{\mu}_k^x, \boldsymbol{\Sigma}_k^{xx})}{\sum_{m=1}^K \alpha_m \mathcal{N}(\mathbf{x}; \boldsymbol{\mu}_m^x, \boldsymbol{\Sigma}_m^{xx})} \quad (4)$$

The converted feature is a weighted sum of component-wise affine transforms:

$$\hat{\mathbf{y}} = F(\mathbf{x}) = \sum_{k=1}^K p(k|\mathbf{x}) \{ \boldsymbol{\mu}_k^y + \boldsymbol{\Sigma}_k^{yx} (\boldsymbol{\Sigma}_k^{xx})^{-1} (\mathbf{x} - \boldsymbol{\mu}_k^x) \} \quad (5)$$

2.3. Mathematical relationship between SSL-GMMVC and LinearVC

SSL-GMMVC can be viewed as an extension of LinearVC that replaces a single global mapping with a mixture of locally linear mappings. Setting $K = 1$ in (5) gives $p(k = 1|\mathbf{x}) = 1$, reducing the conversion to the affine transform:

$$F(\mathbf{x}) = \boldsymbol{\mu}^y + \boldsymbol{\Sigma}^{yx} (\boldsymbol{\Sigma}^{xx})^{-1} (\mathbf{x} - \boldsymbol{\mu}^x) \quad (6)$$

Letting $\mathbf{W} = (\boldsymbol{\Sigma}^{xx})^{-1} \boldsymbol{\Sigma}^{yx}$ and $\mathbf{b} = \boldsymbol{\mu}^y - \mathbf{W}^\top \boldsymbol{\mu}^x$ gives $F(\mathbf{x}) = \mathbf{W}^\top \mathbf{x} + \mathbf{b}$, which is mathematically equivalent to LinearVC. For $K > 1$, each component applies a different affine transform, yielding a locally linear but globally nonlinear mapping that captures local structure.

3. Voice conversion experiments

3.1. Data

We used American English speech from CMU ARCTIC [23], selecting three male (bdl, rms, aew) and three female (slt, clb, lnh) speakers. Each utterance was around 2–3 seconds long.

3.2. Implementation of SSL-GMMVC

Following [19, 20], we extracted 1024-dimensional SSL features from the 6th layer of WavLM-Large [12], which mainly captures speaker information, using 20 ms frames from 16 kHz audio. We aligned source and target features via bidirectional cosine-similarity nearest-neighbor matching. GMM training followed section 2.2 with two covariance variants: *Full* (F), where the covariance matrix is unconstrained, and *Cross Diag* (CD), where all four blocks in (2) are diagonal. CD was widely used in traditional GMM-VC to prevent overfitting and was included here to examine model complexity effects. Waveforms were synthesized with a HiFi-GAN [24] vocoder trained by [19] to accept WavLM-Large 6th-layer features².

3.3. VC models for evaluation

We compared SSL-GMMVC variants and baselines across training-set sizes of $N \in \{10, 20, 50, 100, 200, 300\}$ utterances. SSL-GMMVC spanned six configurations combining covariance types F/CD and the number of mixtures $K \in \{1, 2, 4\}$. Since larger K increases the total number of parameters to estimate, which becomes unstable with limited data, we capped K at 4 and required $N \geq 50$ for $K=2$ and $N \geq 100$ for $K=4$ for stable estimation. For LinearVC, we evaluated NC (*No Constraint*; unconstrained affine transform) and BO (*Bias Only*; per-dimension mean shift). As a deep baseline, we used

²github.com/bshall/knn-vc

FreeVC [17], a VITS-based zero-shot model. It is the most comparable model to our approach, as it uses WavLM-Large features and HiFi-GAN synthesis. In preliminary experiments, increasing the number of reference utterances beyond 10 did not improve speaker similarity, so we used 10 throughout.

3.4. Objective evaluation

Setup. For all 30 ordered pairs from 6 speakers, we trained each model and evaluated converted speech in terms of speaker similarity, intelligibility and naturalness. Intelligibility and naturalness were evaluated on 40 utterances not used for training.

Speaker similarity. We computed equal error rate (EER) using a speaker verifier that scores ECAPA-TDNN [25] embeddings by cosine similarity³. We evaluated discrimination between 100 converted–real pairs (converted speech vs. real target speech) and 100 real–real pairs, constructed with different linguistic content. Higher EER (up to 50%) indicates higher similarity to the target speaker.

Intelligibility. We transcribed converted speech with Whisper-base⁴ [26] and reported word error rate (WER) against the ground-truth. Lower WER indicates higher intelligibility.

Naturalness. We estimated perceived naturalness using UT-MOS [27], a mean opinion score (MOS) prediction model.

3.5. Subjective evaluation

Setup. We conducted listening tests on four speaker pairs covering all gender directions (bdl→rms, clb→slt, bdl→slt, and clb→rms). We converted five utterances per model for each pair and collected five ratings per sample via the crowdsourcing platform Lancers. We report the mean opinion scores (MOS) of speaker similarity and naturalness.

Speaker similarity. Raters scored similarity to the target speaker on a 4-point scale. Each trial presented a reference utterance (real target speech) and an evaluation utterance with different linguistic content, followed by a rating. Each rater evaluated 21 trials in random order. As an attention check, we included one real–real same-speaker trial and excluded raters who rated it as 1.

Naturalness. Raters scored naturalness on a 5-point scale (5 = most natural) by listening to each utterance in isolation. Each rater evaluated 21 samples in random order using the same attention check as for speaker similarity.

4. Results

4.1. Results of the objective evaluation

Table 1 summarizes the objective evaluation results. Because FreeVC is pretrained, its performance is independent of training-set size. We refer to SSL-GMMVC F and LinearVC NC collectively as *unconstrained* models, and SSL-GMMVC CD and LinearVC BO as *constrained* models.

Speaker similarity. The EER of SSL-GMMVC F increased steadily with training data size, surpassing LinearVC NC at $N \geq 100$ for $K=2$ and at $N \geq 200$ for $K=4$. This confirms that more mixture components enable the model to more effectively exploit larger training sets. SSL-GMMVC CD consistently outperformed LinearVC BO across all configurations, despite both resulting in comparatively low EERs. This advantage stems from CD learning both scaling and shifting, while BO is limited to shifting alone. For CD , EER rose by 1.0–1.5% per step as K

³huggingface.co/speechbrain/spkrec-ecapa-voxceleb

⁴github.com/openai/whisper

Table 1: Objective evaluation results of speaker similarity, intelligibility and naturalness. N is the number of training utterances. Underline indicates SSL-GMMVC values that surpass FreeVC. Bold indicates SSL-GMMVC F with $K=2$ or $K=4$ matching or exceeding LinearVC NC at the same N .

Model	EER [%] (\uparrow)							WER [%] (\downarrow)							UTMOS (\uparrow)					
	K	N						N							N					
		10	20	50	100	200	300	10	20	50	100	200	300	10	20	50	100	200	300	
SSL-GMMVC	F	1	9.58	22.73	26.40	26.42	25.78	25.77	12.14	3.64	2.91	2.71	2.63	2.70	3.08	4.12	4.28	4.32	4.33	4.33
		2	–	–	25.00	26.47	27.27	26.37	–	–	3.06	2.98	2.81	2.85	–	–	4.23	4.31	4.33	4.33
		4	–	–	–	26.02	27.30	27.35	–	–	–	3.03	2.95	2.79	–	–	–	4.26	4.31	4.33
	CD	1	2.00	2.07	1.77	1.67	1.57	1.73	3.10	3.16	3.13	3.08	3.05	3.00	4.01	4.03	4.06	4.07	4.08	4.08
		2	–	–	3.27	2.97	3.07	2.92	–	–	3.10	3.01	3.04	3.12	–	–	4.07	4.09	4.10	4.11
		4	–	–	–	4.40	4.20	4.22	–	–	–	3.18	3.00	3.07	–	–	–	4.11	4.13	4.13
LinearVC	NC	–	9.58	22.77	26.45	26.40	25.88	25.73	12.20	3.71	2.93	2.80	2.61	2.70	3.08	4.12	4.28	4.32	4.33	4.33
	BO	–	0.73	0.62	0.65	0.73	0.67	0.62	3.24	3.25	3.24	3.25	3.22	3.28	4.07	4.07	4.08	4.08	4.08	4.08
FreeVC	–	–	–	2.85	–	–	–	–	–	3.85	–	–	–	–	–	4.25	–	–	–	–

increased, confirming that the increase in the number of mixtures yields consistent gains even under covariance constraints. Overall, all SSL-GMMVC models except CD at $K=1$ achieved higher EER than FreeVC.

Intelligibility. *Unconstrained* models showed elevated WER at $N=10$ but fell below FreeVC at $N \geq 20$. SSL-GMMVC F did not surpass LinearVC NC in intelligibility, but remained closely comparable. *Constrained* models remained intelligible even with $N=10$, with SSL-GMMVC CD outperforming LinearVC BO across all settings. This likely reflects their smaller parameterization, which learns content-preserving mappings more reliably from limited data while limiting speaker resemblance.

Naturalness. In the *unconstrained* setting, SSL-GMMVC F with $K > 1$ reached naturalness on par with LinearVC NC and above FreeVC at $N \geq 200$, confirming that the GMM transformation preserves the naturalness of SSL features. In the *constrained* setting, SSL-GMMVC CD with $K > 1$ consistently surpassed LinearVC BO at $N \geq 100$, and even CD at $K=1$ maintained stable naturalness across all training-set sizes.

4.2. Results of the subjective evaluation

Table 2 reports the subjective evaluation results.

Speaker similarity. With $N \geq 20$, all *unconstrained* models surpassed FreeVC, and MOS increased with larger training data. SSL-GMMVC F exceeded LinearVC NC at $N \geq 200$, broadly consistent with the objective results. In the *constrained* settings, SSL-GMMVC CD consistently surpassed LinearVC BO and improved with larger K , aligning with the objective findings. At $N=10$, however, *unconstrained* models fell below FreeVC due to conversion artifacts from insufficient data.

Naturalness. *Unconstrained* models showed low naturalness at $N=10$ due to conversion artifacts, but recovered sharply with $N \geq 20$ and approached FreeVC-level naturalness as training-set size increased. *Constrained* models, by contrast, maintained stable naturalness across all training-set sizes, consistent with the objective results.

5. Further analysis

This section investigates how mixture components relate to phonetic categories and how the transformation matrices act on the feature space across speaker pairs.

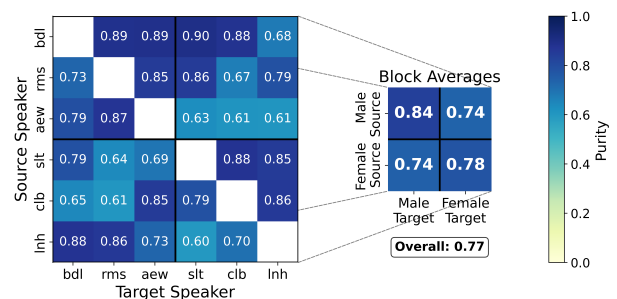


Figure 2: Purity between mixture selection and sonority (left: speaker pairs; right: gender-pair averages).

5.1. Component selection

5.1.1. Setup

We analyzed SSL-GMMVC F ($K=2$, $N=200$) with 50 held-out utterances per speaker pair. Frames were labeled as sonorants or obstruents [28, Chapter 5] via Montreal Forced Aligner [29], and purity [30] was computed using posteriors (4) as soft assignments, where $\mathcal{C} = \{\text{son, obs}\}$ and T is the number of non-silent frames:

$$\text{Purity} = \frac{1}{T} \sum_k \max_{c \in \mathcal{C}} \sum_{t: c_t=c} p(k|\mathbf{x}_t) \quad (7)$$

5.1.2. Results

Figure 2 showed a relatively high overall purity, indicating the correlation between mixture selection and sonority, though variation existed across pairs. More specifically, same-gender conversions tended to achieve higher purity than cross-gender ones.

5.2. Transformation matrices

5.2.1. Setup

Using the same evaluation set, we analyzed SSL-GMMVC F ($K=1$, $N=200$). We computed mean per-frame cosine angles between source and converted SSL features across all, sonorant, and obstruent regions. However, identical angles can correspond to very different directions in 1024-dimensional space,

Table 2: Subjective evaluation results of speaker similarity and naturalness (MOS with 95% confidence interval in parentheses). N indicates the number of training utterances. Underline indicates SSL-GMMVC values that surpass FreeVC. Bold indicates SSL-GMMVC F with $K=2$ or $K=4$ matching or exceeding LinearVC NC at the same N .

Model	K	Speaker similarity (\uparrow)						Naturalness (\uparrow)						
		N						N						
		10	20	50	100	200	300	10	20	50	100	200	300	
SSL-GMMVC	F	1	1.91(18)	2.42(19)	2.64(20)	2.76(19)	2.97(19)	2.84(21)	2.51(22)	3.75(23)	4.00(21)	3.94(21)	3.99(20)	4.07(19)
		2	–	–	2.67(20)	2.80(17)	2.88(18)	2.90(19)	–	–	3.92(19)	4.00(18)	3.97(18)	4.09(19)
		4	–	–	–	2.74(19)	2.65(19)	2.85(18)	–	–	–	4.01(20)	3.96(18)	4.10(18)
	CD	1	2.02(20)	1.84(19)	2.00(19)	1.87(19)	1.93(18)	2.05(22)	3.70(21)	3.66(20)	3.61(20)	3.72(22)	3.93(20)	3.84(20)
		2	–	–	2.17(21)	2.25(18)	2.17(18)	2.03(19)	–	–	3.74(20)	3.60(20)	3.82(20)	3.85(19)
		4	–	–	–	2.29(21)	2.35(21)	2.19(21)	–	–	–	3.79(20)	3.46(20)	3.94(21)
LinearVC	NC	–	1.59(16)	2.45(20)	2.63(20)	2.87(20)	2.75(20)	2.64(19)	2.33(22)	3.74(20)	4.02(20)	3.90(20)	4.05(19)	4.21(18)
	BO	–	1.71(18)	1.64(16)	1.84(20)	1.73(18)	1.58(18)	1.58(16)	3.72(21)	3.70(22)	3.68(23)	3.81(22)	3.54(24)	3.77(22)
FreeVC	–	–	–	2.04(20)	–	–	–	–	–	4.11(18)	–	–	–	

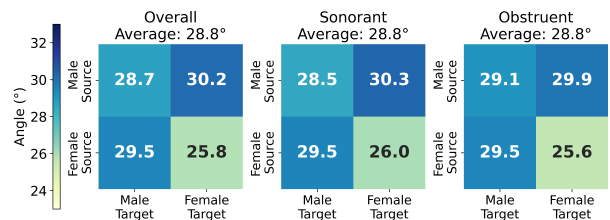


Figure 3: Average per-frame cosine angles between source and converted SSL features reported for each gender direction and for all / sonorant / obstruent regions.

so angles alone cannot reveal the global transformation structure. We therefore additionally analyzed the eigenvalues of the conversion matrix \mathbf{W} from subsection 2.3. For an eigenvalue $\lambda = r e^{i\theta}$, r captures scaling and θ captures the angle of the corresponding rotational plane [31]. Although our primary contribution is the multi-component formulation, we restricted this analysis to $K=1$. For $K>1$, quantitative comparison of per-component spectra is not yet established, as it requires matching rotational planes across components, for which no principled method exists. Thus, we provided an interpretable characterization of the general transformation using a single-component model.

5.2.2. Results

Figure 3 showed cosine angles typically in the 25–30° range. Female→female had the smallest angles, followed by male→male, then cross-gender pairs, with no clear difference between sonorants and obstruents. Figure 4 shows the (r, θ) spectra of eigenvalues sorted by descending r for the four speaker pairs from subsection 3.5. Planes with high r typically had small rotation angles, while low r showed larger variability but contributed less due to strong shrinkage. Thus, the transformation is a contractive rotation, concentrating information in few components. In addition, the clb→slt pair showed smaller rotation angles, consistent with the female→female trend in Figure 3. This tentatively suggests that θ may reflect inter-speaker acoustic distance, though this warrants further investigation.

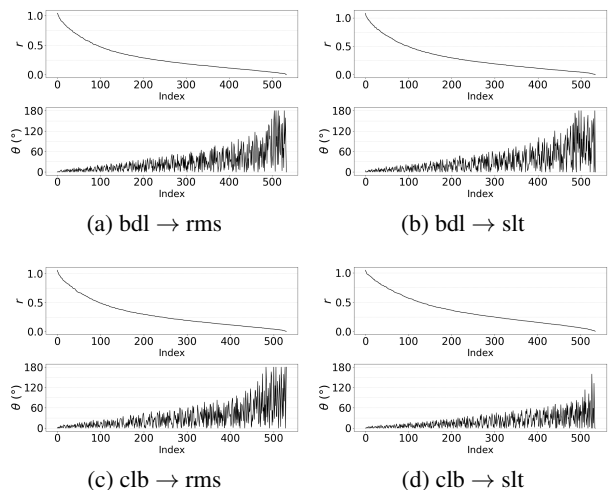


Figure 4: Spectra of eigenvalues of the conversion matrix for representative speaker pairs.

6. Conclusion

We presented SSL-GMMVC, a GMM-based voice conversion method that extends a single global transform to locally linear mappings in SSL feature space. Objective and subjective evaluations showed that SSL-GMMVC improves speaker similarity over LinearVC in particular settings with comparable intelligibility and naturalness. Even the constrained covariance variant with multiple components surpassed FreeVC in speaker similarity when increasing the number of components. Further analysis revealed that mixture component selection correlates with phonetic structure, and that the learned transforms are characterized as contractive rotations, with angles tentatively suggesting a relationship to inter-speaker acoustic distance. However, scaling the number of mixture components while maintaining stable parameter estimation in high-dimensional SSL space remains an open challenge, and the rotation-spectrum analysis does not yet establish correspondences between rotational planes across speaker pairs. Future work includes addressing these limitations and further exploring the structure of SSL representations through the lens of VC.

7. Acknowledgements

This research was supported by JSPS KAKENHI Grant Number JP25K22829. The authors would like to thank Kentaro Onda at The University of Tokyo, for his valuable assistance in refining this work.

8. Use of generative AI tools

GPT-5.2 was used to aid editing and polishing this manuscript.

9. References

- [1] D. G. Childers, K. Wu, D. Hicks, and B. Yegnanarayana, "Voice conversion," *Speech Communication*, vol. 8, no. 2, pp. 147–158, 1989.
- [2] B. M. L. Srivastava, N. Vauquier, M. Sahidullah, A. Bellet, M. Tommasi, and E. Vincent, "Evaluating voice conversion-based privacy protection against informed attackers," in *ICASSP 2020-2020 IEEE International Conference on Acoustics, Speech and Signal Processing (ICASSP)*. IEEE, 2020, pp. 2802–2806.
- [3] H.-P. Chang, I.-C. Yoo, C. Jeong, and D. Yook, "Zero-shot unseen speaker anonymization via voice conversion," *IEEE Access*, vol. 10, pp. 130 190–130 199, 2022.
- [4] D. Felps, H. Bortfeld, and R. Gutierrez-Osuna, "Foreign accent conversion in computer assisted pronunciation training," *Speech communication*, vol. 51, no. 10, pp. 920–932, 2009.
- [5] H. Geng, D. Saito, and N. Minematsu, "A pilot study of applying sequence-to-sequence voice conversion to evaluate the intelligibility of 12 speech using a native speaker's shadowings," in *2024 Asia Pacific Signal and Information Processing Association Annual Summit and Conference*, 2024, pp. 1–6.
- [6] K. Nakamura, T. Toda, H. Saruwatari, and K. Shikano, "Speaking-aid systems using gmm-based voice conversion for electrolaryngeal speech," *Speech communication*, vol. 54, no. 1, pp. 134–146, 2012.
- [7] M. Illa, B. M. Halpern, R. van Son, L. Moro-Velazquez, and O. Scharenborg, "Pathological voice adaptation with autoencoder-based voice conversion," in *11th ISCA Speech Synthesis Workshop (SSW 11)*, 2021, pp. 19–24.
- [8] S. H. Mohammadi and A. Kain, "An overview of voice conversion systems," *Speech Communication*, vol. 88, no. C, pp. 65–82, Apr. 2017.
- [9] B. Sisman, J. Yamagishi, S. King, and H. Li, "An overview of voice conversion and its challenges: From statistical modeling to deep learning," *IEEE/ACM Transactions on Audio, Speech, and Language Processing*, vol. 29, pp. 132–157, 2020.
- [10] A. Baevski, Y. Zhou, A. Mohamed, and M. Auli, "wav2vec 2.0: A framework for self-supervised learning of speech representations," in *Advances in Neural Information Processing Systems*, vol. 33. Curran Associates, Inc., 2020, pp. 12 449–12 460.
- [11] W.-N. Hsu, B. Bolte, Y.-H. H. Tsai, K. Lakhota, R. Salakhutdinov, and A. Mohamed, "HuBERT: Self-supervised speech representation learning by masked prediction of hidden units," *IEEE/ACM Transactions on Audio, Speech, and Language Processing*, vol. 29, pp. 3451–3460, 2021.
- [12] S. Chen, C. Wang, Z. Chen, Y. Wu, S. Liu, Z. Chen, J. Li, N. Kanda, T. Yoshioka, X. Xiao, J. Wu, L. Zhou, S. Ren, Y. Qian, Y. Qian, J. Wu, M. Zeng, X. Yu, and F. Wei, "WavLM: Large-scale self-supervised pre-training for full stack speech processing," *IEEE Journal of Selected Topics in Signal Processing*, vol. 16, no. 6, pp. 1505–1518, Oct. 2022.
- [13] S. Liu, A. Mallol-Ragolta, E. Parada-Cabaleiro, K. Qian, X. Jing, A. Kathan, B. Hu, and B. W. Schuller, "Audio self-supervised learning: A survey," *Patterns*, vol. 3, no. 12, 2022.
- [14] A. Mohamed, H.-y. Lee, L. Borgholt, J. D. Havtorn, J. Edin, C. Igel, K. Kirchhoff, S.-W. Li, K. Livescu, L. Maaløe, T. N. Sainath, and S. Watanabe, "Self-supervised speech representation learning: A review," *IEEE Journal of Selected Topics in Signal Processing*, vol. 16, no. 6, pp. 1179–1210, 2022.
- [15] S. wen Yang, P.-H. Chi, Y.-S. Chuang, C.-I. J. Lai, K. Lakhota, Y. Y. Lin, A. T. Liu, J. Shi, X. Chang, G.-T. Lin, T.-H. Huang, W.-C. Tseng, K. tik Lee, D.-R. Liu, Z. Huang, S. Dong, S.-W. Li, S. Watanabe, A. Mohamed, and H. yi Lee, "SUPERB: Speech processing universal performance benchmark," in *Interspeech 2021*, 2021, pp. 1194–1198.
- [16] W.-C. Huang, S.-W. Yang, T. Hayashi, H.-Y. Lee, S. Watanabe, and T. Toda, "S3PRL-VC: Open-source voice conversion framework with self-supervised speech representations," in *ICASSP 2022 - 2022 IEEE International Conference on Acoustics, Speech and Signal Processing (ICASSP)*, 2022, pp. 6552–6556.
- [17] J. Li, W. Tu, and L. Xiao, "Freevc: Towards high-quality text-free one-shot voice conversion," in *ICASSP 2023-2023 IEEE International Conference on Acoustics, Speech and Signal Processing*, 2023, pp. 1–5.
- [18] J. Kim, J.-H. Kim, Y. Choi, T. D. Nguyen, S. Mun, and J. S. Chung, "AdaptVC: High quality voice conversion with adaptive learning," in *ICASSP 2025-2025 IEEE International Conference on Acoustics, Speech and Signal Processing (ICASSP)*. IEEE, 2025, pp. 1–5.
- [19] M. Baas, B. van Niekerk, and H. Kamper, "Voice conversion with just nearest neighbors," in *Proc. Interspeech 2023*, 2023, pp. 2053–2057.
- [20] H. Kamper, B. van Niekerk, J. Zaïdi, and M.-A. Carbonneau, "LinearVC: Linear transformations of self-supervised features through the lens of voice conversion," in *Proc. Interspeech 2025*, 2025, pp. 1398–1402.
- [21] A. Sichertman and Y. Adi, "Analysing discrete self supervised speech representation for spoken language modeling," in *ICASSP 2023-2023 IEEE International Conference on Acoustics, Speech and Signal Processing (ICASSP)*. IEEE, 2023, pp. 1–5.
- [22] Y. Stylianou, O. Cappé, and E. Moulines, "Continuous probabilistic transform for voice conversion," *IEEE Transactions on Speech and Audio Processing*, vol. 6, no. 2, p. 131, 1998.
- [23] J. Kominek and A. W. Black, "The CMU ARCTIC speech databases," in *5th ISCA Workshop on Speech Synthesis*, 2004, pp. 223–224.
- [24] J. Kong, J. Kim, and J. Bae, "HiFi-GAN: Generative adversarial networks for efficient and high fidelity speech synthesis," *Advances in Neural Information Processing Systems*, vol. 33, pp. 17 022–17 033, 2020.
- [25] B. Desplanques, J. Thienpondt, and K. Demuynck, "ECAPA-TDNN: Emphasized channel attention, propagation and aggregation in tdn based speaker verification," in *Proc. Interspeech 2020*, 2020, pp. 3830–3834.
- [26] A. Radford, J. W. Kim, T. Xu, G. Brockman, C. McLeavey, and I. Sutskever, "Robust speech recognition via large-scale weak supervision," in *International conference on machine learning*. PMLR, 2023, pp. 28 492–28 518.
- [27] T. Saeki, D. Xin, W. Nakata, T. Koriyama, S. Takamichi, and H. Saruwatari, "UTMOS: UTokyo-SaruLab System for Voice-MOS Challenge 2022," in *Proc. Interspeech 2022*, 2022, pp. 4521–4525.
- [28] D. A. Burquest, *Phonological Analysis: A Functional Approach*, 3rd ed. Summer Institute of Linguistics, 2006.
- [29] M. McAuliffe, M. Socolof, S. Mihuc, M. Wagner, and M. Sonderegger, "Montreal forced aligner: Trainable text-speech alignment using kaldia," in *Proc. Interspeech 2017*, 2017, pp. 498–502.
- [30] W.-H. Tsai, S.-S. Cheng, and H.-M. Wang, "Speaker clustering of speech utterances using a voice characteristic reference space," in *Proc. Interspeech 2004*, 2004, pp. 2937–2940.
- [31] D. Saito, N. Minematsu, and K. Hirose, "Rotational properties of vocal tract length difference in cepstral space," *Journal of Research Institute of Signal Processing*, vol. 15, no. 5, pp. 363–374, 2011.